Interpretation of Laser Absorption Measurements on 4H-SiC Bipolar Diodes by Numerical Simulation

D. Werber and G. Wachutka
Institute for Physics of Electrotechnology
Munich University of Technology
Munich, Germany
werber@tep.ei.tum.de, wachutka@tep.ei.tum.de

***Abstract*—The interpretation and evaluation of free carrier absorption experiments on SiC devices is essentially supported by computer simulations of the measurement process, which exploits the physical effect that the light absorption coefficient in a semiconductor depends on the electron and hole concentrations. Hence, the attenuation of a laser beam transmitted through a sample is an integral function of the local charge carrier density along the optical path. We investigated time-resolved absorption profiles in 4H-SiC pin-diodes in the high-injection regime at current densities of 100 A/cm². Based on "virtual experiments" we studied the factors limiting the spatial resolution or disturbing the absorption signal such as Fabry-Perot interferences.**

Keywords-4H-SiC bipolar diode, device simulation, virtual experiment, free carrier absorption,

I. INTRODUCTION

Commonly high power devices are experimentally characterized by their electrical terminal behavior, while the "innerelectronic" behavior is amenable to theoretical analysis or computer simulation only. But with a view to optimizing the device properties a detailed view into the interior of real devices under real operation conditions is highly desirable. This motivated us to set up an experimental platform for the direct space- and time-resolved measurement of carrier profiles using a laser-aided probing technique, which exploits the plasma-optical effect, i.e. the sensitivity of the complex refractive index to the carrier concentrations [1]. The correct interpretation of the measured light absorption and deflection signals is quite involved and requires an accurate physical model of the measurement process itself. Equipped with that, we performed virtual numerical experiments consisting of three parts: electrothermal device simulation, calculation of the light propagation and of the detector responses. Comparing the results of real and virtual experiments allows us to correctly evaluate the measured raw data and, at the same time, to calibrate the underlying physical device models.

II. EXPERIMENTAL

A. Plasma-Optical Effect

A semi-classical description of the plasma-optical effect for quasi-free charge carriers in conducting solids is the well-known Drude model, which assumes harmonic oscillators with vanishing binding energies for the charge carriers. The resulting light absorption coefficient is modulated by a factor α, which depends linearly on the charge carrier concentrations of electrons n and holes p:

$$\alpha = \frac{q^3\lambda^2}{4\pi^2\varepsilon_0 n_r c^3}\left(\frac{n}{m_n^{*2}\mu_n}+\frac{p}{m_p^{*2}\mu_p}\right) \tag{1}$$

Here, n_r denotes the static refractive index, q the electron charge, λ the light wavelength, ε_0 the dielectric constant, c the speed of light, $m^*_{n/p}$ the effective masses of the carriers, and $\mu_{n/p}$ their mobilities.

For low carrier concentrations this contribution to the light absorption is only a small fraction compared to that caused by the host lattice, whereas in heavily doped regions the carrier-induced absorption rises by many orders of magnitude. Consequently the transmission of light is drastically reduced to such a low level that the transmitted light intensity may fall below the detection threshold of the sensor circuit.

Assuming that carrier-carrier scattering has a minor influence on the carrier mobilites, the mobilities $\mu_n(x)$ and $\mu_p(x)$ in the intrinsic region of the pin diode have constant values under isothermal conditions. Using model parameters for SiC, equation (1) results for a laser wavelength of 405 nm in

$$\alpha = 5.10\cdot 10^{-20}\ \mathrm{cm}^2\cdot n + 5.78\cdot 10^{-20}\ \mathrm{cm}^2\cdot p\,. \tag{2}$$

B. Measurement Principle

A strongly focused light beam is transmitted through a 4H-SiC pin diode, which is operated in pulsed mode (i.e. periodically turned on and off) (c.f. Fig. 1). The light absorption in the sample is measured by a very fast photo-diode circuit. To obtain the whole absorption profile in the low-doped intrinsic region of the device, the laser beam is parallel-shifted in lateral direction relative to the device. The light absorption ΔI during the on-state of the pin diode is quantified by the relative difference of the transmitted light intensities between on- and off-state:

$$\Delta I = I_{on,trans} - I_{off,trans} \tag{3}$$

The absorption ΔI is a function of the carrier density induced

modification of the absorption coefficient and the sample length L:

$$\Delta I = (e^{-\Delta\alpha L} - 1)\, I_{off,trans} \quad (4)$$

The interpretation of the absorption profiles is considerably facilitated, if the diode is driven close to high-injection conditions. In this case, the excess carrier concentrations $\Delta n(x)$ and $\Delta p(x)$ in the intrinsic region of the device obey approximately the relations

$$\Delta p(x) \approx p(x) = n(x) - N_D^+(x) \approx \Delta n(x) \quad (5)$$

The concentration of the ionized donors, $N_D^+(x)$, cannot be neglected in the charge balance, not even for high current rates, because the carrier density modulation in the intrinsic region is small due to the short minority carrier lifetime. With eq. (5) the modification of the absorption coefficient $\Delta\alpha$ can be expressed as

$$\Delta\alpha(x) = 1.09 \cdot 10^{-19}\,\mathrm{cm}^2 \cdot \Delta n(x) \quad (6)$$

A Taylor expansion of eq. (4) together with eq. (6) leads to a linear dependence of the light absorption and the excess carrier density.

$$\Delta I(x) \sim -\Delta\alpha(x) \sim -\Delta n(x) \approx -\Delta p(x) \quad (7)$$

With an ideal optical geometry neglecting the beam profile of the laser beam, the absorption profile $\Delta I(x)$ would directly correlate with the excess carrier densities in the intrinsic region of the bipolar diode. The relative shape of the carrier profiles could be directly extracted from measuring the position-dependent variation of the light absorption. However, for the real experimental conditions, the extraction of the excess carrier densities from the light absorption signal becomes quite involved and cannot be done without the assistance of computer simulations ("virtual experiments").

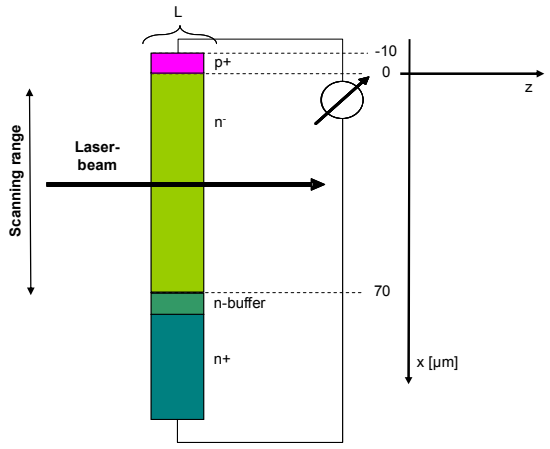

Figure 1. Light is transmitted through a bipolar diode with sample length L. The diode is operated in pulsed mode

C. Test Samples

The devices under test were 4H-SiC pin diodes, especially manufactured by SiCED for this purpose [2]. They have a low-doped intrinsic region with a nitrogen doping concentration of $1.4 \cdot 10^{15}$ cm^{-3} and a thickness of 70 µm, and an enlarged Al-implanted p-emitter with a p-doping of about 10^{19} cm^{-3} and a thickness of 10 µm, whereas regular diodes exhibit a p-emitter thickness of 3 µm only. With this enlarged p-emitter it is possible to measure the absorption also in the vicinity of the pn-junction without any interfering refractions at the electric contact. The electronic behaviour of the diode did not show any significant change by this modification [3]. The original devices are sawn into thin slices with a nominal thickness of approximately 500 µm. In order to suppress light scattering at the lateral surfaces of the samples, they are diamond-polished in a sequence of four steps, until these surfaces are optically smooth (i.e. surface roughness $R_q < \lambda/8$). Moreover, this special treatment of the samples ensures co-planarity of the two side faces. After the preparation process the sample thickness amounts about 200 µm.

The samples are turned on and off by current pulses of adjustable pulse width and current level. The duty cycle is chosen as small as possible to avoid disturbing effects such as self-heating of the sample.

D. Limiting and Disturbing Effects

1) Spatial resolutions: Illuminating a volume by the laser beam, the finite width of the beam profile causes a limitation of the spatial resolution of the absorption signal. More precisely, the position-dependent modulation of the intensity of the transmitted light $\Delta I(x)$ can be expressed as convolution integral of the excess carrier distribution $\Delta c(x)=\Delta n(x)=\Delta p(x)$ in the electron-hole plasma with the spatial sensitivity function $A(x)$ of the measurement setup:

$$\Delta I(x) = \int A(x-\xi)\, \Delta c(\xi)\, d\xi \quad (9)$$

2) Fabry-Perot interferences: With its two parallel side faces the sample constitutes (unintentionally) a Fabry-Perot resonator. When it is penetrated by coherent laser light, optical interferences occur which modulate the transmitted light intensity $\Delta I(x)$ in addition to the plasma-optical effect. Self-heating of the device under test during a measurement sequence leads to a temperature-induced change of the optical refractive index which, in turn, causes a change of the transmittivity of the Fabry-Perot resonator. This complicates or may even prevent the extraction of the excess charge profile from the absorption signal.

E. Measurement Results

The test samples were subjected to periodic current pulses of 5 µs duration with a duty cycle of 0.01. Light absorption profiles were measured for a current level of 100 A/cm² at different times after the on-set of the current pulse. Fig. 2 shows the time-dependent change of the absorption signal. Only in the intrinsic region 0 µm < x < 70 µm the absorption signal allows a meaningful interpretation. Obviously, the absorption signal changes monotonously with time. One cause for the increase of absorption is the flooding of the intrinsic zone, another one is additional absorption due to temperature-induced variations of the Fabry-Perot cavity.

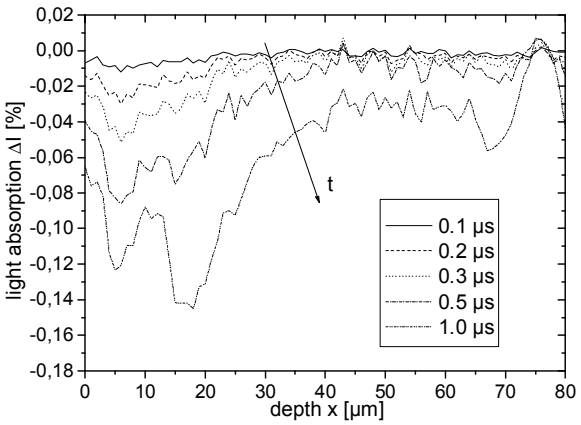

Figure 2. Absorption profiles for a current step of 100 A/cm² at 0.1 µs, 0.2 µs, 0.3 µs, 0.5 µs and 1 µs after the on-set of the current pulse.

III. SIMULATION

For a thorough understanding of the measurement process and a proper interpretation and evaluation of the absorption signal, we performed virtual numerical experiments consisting of three parts, electrothermal device simulation, calculation of the beam propagation and calculation of the detector responses (Fig. 3).

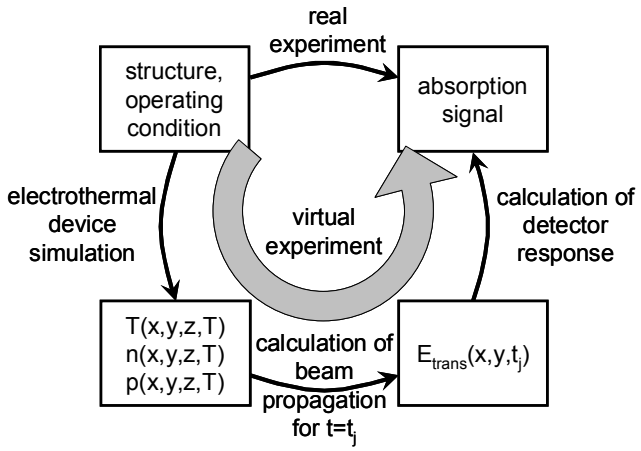

Figure 3. Interrelation of real and virtual experiment, consisting of three subsequent stages.

A. Electrothermal Device Simulation

Transient electrothermal device simulations were carried out using the simulation tool TeSCA [4]. The physical models included Shockley-Read-Hall and Auger recombination, incomplete ionization of the dopants, and the Caughey-Thomas model for the carrier mobilities. In accordance with experimental findings, we set the maximum values of the electron and hole mobilities at room temperature to 800 cm²/Vs and 124 cm²/Vs, respectively. The Shockley-Read-Hall minority carrier lifetimes were chosen as 70 ns for electrons and 14 ns for holes, respectively. Joule heating and recombination heating were included as sources of self-heating.

Applying a current step of 100 A/cm² at t=0 causes flooding of the intrinsic region of the pin diode by electrons and holes, as it is displayed in Fig. 4 (please note that x=0 denotes the location of the pn-junction in all the following graphs.). Evidently, minority carrier injection occurs from the p-emitter. As soon as the hole density approaches the high-injection level, charge neutrality requires that the excess densities of electrons and holes rise in parallel (c.f. eq. (5)). Hence, electron injection from the n-buffer sets on after 0.1 µs. After about t=1µs, the flooding of the i-zone is completed and the modulation of the carrier density profiles becomes stationary.

Fig. 5 shows the time-dependent temperature distributions corresponding to Fig. 4. The heat production mechanisms are recombination heat in the vicinity of the pn-junction and Joule heat in the drift region. Since the thermal time constant is much longer than the period in which the snapshots in Fig. 5 are taken, the temperature distributions are still far from becoming stationary.

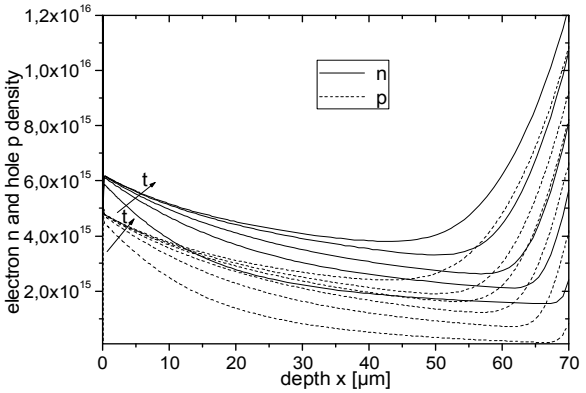

Figure 4. Time-resolved electron (n) and hole (p) densities for a current step of 100 A/cm² at 0.1 µs, 0.2 µs, 0.3 µs, 0.5 µs and 1 µs after turn-on.

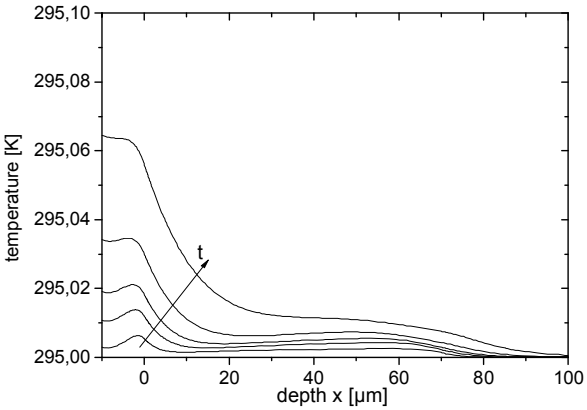

Figure 5. Temperature distributions for a current step of 100 A/cm² at 0.1 µs, 0.2 µs, 0.3µs, 0.5 µs and 1 µs after turn-on.

B. Simulation of the Optical Experiment

At a sequence of time steps t=t_i snapshots of the carrier and temperature distributions in the interior of the pin diode are passed to an in house tool that calculates the beam propagation through the device. After evaluating the local complex optical refractive index the impinging light, modelled as Gaussian beam, is calculated on its way through the sample by means of

a propagation matrix technique [4]. Finally, the detector response is determined for the times $t=t_j$ relatively to the detector response at the time $t=0$.

Figs. 6 and 7 show two sequences of time-dependent calculated detector responses with slightly different sample lengths L and L', with the difference chosen as $\lambda/(8n_r)$. Evidently the absorption signal is quite sensitive to the sample length: The signal in Fig. 6 reflects that a small increase in temperature causes a small variation of the optical length, which has a significant effect on the transmittivity of the Fabry-Perot cavity. In contrast, if the sample length is chosen as a multiple of $\lambda/(4n_r)$, the disturbing influence of the Fabry-Perot interferences is largely suppressed as demonstrated in Fig. 7. The measured absorption profiles in Fig. 2 resemble qualitatively those in Fig. 6, indicating that both of them are strongly affected by Fabry-Perot interferences, whereas the simulated profiles in Fig. 7 are almost free of Fabry-Perot interferences. Since a preparation of the sample length within a tolerance of $\lambda/(8n_r)$ is practically difficult, the disturbance by Fabry-Perot interferences cannot be efficiently suppressed as long as coherent laser light is used for probing.

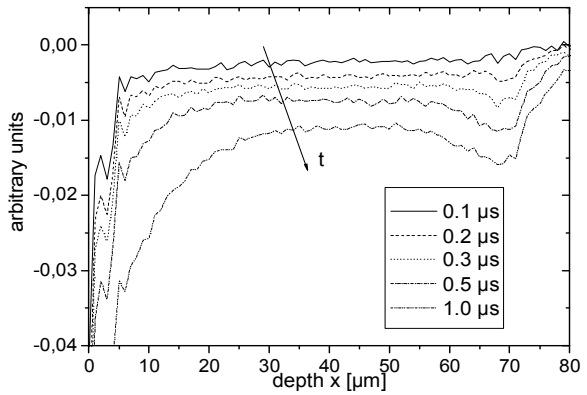

Figure 6. Simulated absoprtion profiles for a current step of 100 A/cm² at 0.1 µs, 0.2 µs, 0.3 µs, 0.5 µs and 1 µs after turn-on.

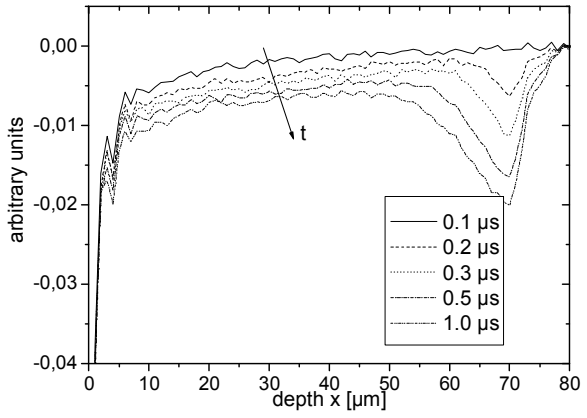

Figure 7. Simulated absoprtion profiles for a current step of 100 A/cm² at 0.1 µs, 0.2 µs, 0.3 µs, 0.5 µs and 1 µs after turn-on with adjusted sample length L'.

IV. Discussion

Despite of the occurrence of the Fabry-Perot interferences, the measured absorption profiles (Fig. 2) contain detailed information on the carrier and temperature distribution in the device, which has to be extracted by an accurate analysis of the optical beam propagation. This reveals, for instance, that the additional absorption maximum for 15 µm<x<20 µm can be attributed to a local variation of the sample length causing destructive interference in the Faby-Perot resonator. Having the optical model validated the measured absorption signal can be corrected for the optical disturbances. Hence, a quantitative comparison between real and virtual experiment becomes possible, which enables the recalibration of the electrical and thermal model parameters and, thus, allow for an accurate predictive simulation of 4H-SiC devices.

V. Conclusion and Perspectives

Free carrier absorption measurements have proven to be a useful diagnosis technique for studying the electrical properties of 4H-SiC bipolar diodes. The interpretation of the measurement results requires the support by virtual experimentation, revealing among others the effect of Fabry-Perot interferences in consequence of self-heating. Nevertheless, comparing the results of real and virtual experiment, we are able to confirm the physical models applied to the device simulation and their parameter values for the material 4H-SiC

In order to simplify the interpretation of the measured absorption profiles, the Fabry-Perot interferences have to be suppressed. To this end, two countermeasures seem feasible: Using an incoherent, but yet strongly confined light beam or, alternatively, employing parallel-polarized light, which prevents reflections under the Brewster-angle.

Acknowledgment

We would like to thank P. Friedrichs, W. Bartsch and H. Mitlehner (SiCED GmbH, Germany) for their assistance and technical support, in particular for supplying us with the 4H-SiC pin-diodes used as DUTs.

References

[1] D. Werber et al, “Investigation on the internal carrier distribution in 4H-SiC pin diodes by laser absorption measurements,” Proc. ICSCRM 2007, Otsu, Japan.

[2] W. Bartsch. et al, “SiC power diodes: design and performance,” Proc. EPE 2007, Aalborg, Denmark.

[3] D. Werber and G. Wachutka, “Numerical design study on the optimal p-emitter thickness of 4H-SiC bipolar diodes,” Proc. SISPAD `07 (Vienna, 2007), ISBN 978-3-211-72860-4 .

[4] developed by Weierstrass-Institute, Berlin, Germany (www.wias-berlin.de).

[5] R. Thalhammer and G. Wachutka, “Virtual optical experiments. part I. modeling the measurement process,” J. Opt. Soc. Am. A, vol. 20, pp. 698-705, April 2003.